

## THE EFFECTS OF TOPOGRAPHY ON THE SUMMER ATMOSPHERIC ENERGETICS OF THE NORTHERN HEMISPHERE IN A LOW-RESOLUTION GLOBAL SPECTRAL MODEL

Ni Yunqi (倪允琪)

Department of Atmospheric Sciences, Nanjing University, Nanjing

Bette L. Otto-Bliesner and David D. Houghton

Department of Meteorology, University of Wisconsin,

Madison, WI 53706, U.S.A.

Received September 15, 1986

### ABSTRACT

An analysis is made of the effects of topography on the summer atmospheric energetics of the Northern Hemisphere in a low-resolution global spectral model. The numerical model is a global, spectral, primitive equation model with five equally spaced sigma levels in the vertical and triangular truncation at wavenumber 10 in the horizontal. The model includes comparatively full physical processes.

Each term of the energy budget equations is calculated in four specific latitudinal belts ( $81.11^{\circ}\text{S}$ – $11.53^{\circ}\text{S}$ ;  $11.53^{\circ}\text{S}$ – $11.53^{\circ}\text{N}$ ;  $11.53^{\circ}\text{N}$ – $46.24^{\circ}\text{N}$ ;  $46.24^{\circ}\text{N}$ – $81.11^{\circ}\text{N}$ ) from a five-year simulation with mountains and a one-year simulation without mountains, respectively. Differences between them are compared and statistically tested. The results show that synoptical scale waves transport available potential energy and kinetic energy to long waves and increase conversion from available potential energy of the zonal flow to eddy's and from the eddy kinetic energy to the zonal kinetic energy in region 3 ( $11.53^{\circ}\text{N}$ – $46.24^{\circ}\text{N}$ ) due to mountains; topography intensifies the atmospheric baroclinity in region 3, consequently the baroclinic conversion of atmosphere energy is increased. The seasonal characteristics associated with the summer atmospheric energy source in region 3 are caused by seasonal variation of the solar radiation and the land-ocean contrasts and independent of topographic effects. The mechanism of topographic effects on the increase of long wave kinetic energy is also discussed.

### 1. INTRODUCTION

The numerical study of topographic effects on atmospheric energetics is an important project. Early in 1971, Kasahara and Washington investigated how mountains affected the transport mechanism of energy using six-layer NCAR global atmospheric general circulation model and suggested that the dynamical effect of the earth's orography plays a minor role compared to the thermal effect of continentality except for the south polar. In subsequent simulation with a 12-layer NCAR GCM, Kasahara and Washington (1973) further found that in the simulation with mountains, there were larger vertical transports and amounts of planetary wave energy, particularly wavenumber 1, in the stratosphere. Manabe and Terpstra (1974)'s experiments indicated that the mountains increased conversion from

potential energy to stationary component of the eddy kinetic energy, therefore, kinetic energy of stationary disturbances was increased and transient eddy component decreased with little effect on the sum of the stationary and transient eddy kinetic energy. With a low-resolution global spectral model, Ni et al. (1986) investigated the effects of topography on global atmospheric energetics and their seasonal variation and found that in summer, mountains increased eddy activities and baroclinic instability of the Northern Hemisphere and gave rise to increasing eddy components of atmospheric energy and conversion from eddy available potential energy to eddy kinetic energy; in winter, topography increased the zonal kinetic energy. The above results revealed the common mechanism of topographic effects on atmospheric energetics. But in summer, the most important atmosphere phenomenon is the monsoonal circulation of planetary scale in the Northern Hemisphere. Some of their members, such as Southern Asian High, Southern Asian Low and Pacific Subtropical High, are located in the northern subtropical zone and its influence scope may even extend to extratropical region (Krishnamurti, 1981; Tao, 1983; Wang, 1986). However, these members of the monsoonal circulation can be identified as quasi-stationary waves of low wavenumber (Murakami, 1981; Webster, 1978). Therefore, analyzing topographic effects on energy of low wavenumber waves in the latitudes during summer has an important significance for understanding the formation and maintenance of the monsoonal circulation.

Murakami (1981) investigated the atmospheric energetics at 200 hPa in four selected latitudinal belts ( $30.8^{\circ}\text{N}$ – $44.6^{\circ}\text{N}$ ;  $14.8^{\circ}\text{N}$ – $30.8^{\circ}\text{N}$ ;  $0^{\circ}$ – $14.8^{\circ}\text{N}$ ;  $14.8^{\circ}\text{S}$ – $0^{\circ}$ ) during three summers in 1970–72 and got significant results. In this study, each term of the energy budget equations in four specific latitudinal belts (see Section II) is calculated from a five-year simulation with mountains and a one-year simulation without mountains, respectively. Differences between results with mountains and without mountains are statistically tested in order to discuss the effects of topography on atmospheric energetics in latitudinal zones, especially in region 3 ( $11.53^{\circ}\text{N}$ – $46.24^{\circ}\text{N}$ ). In Section II, the model and the energy equations used are reviewed. The effects of topography on interaction between waves or between waves and the zonal flow during summer are discussed in Section III. In Section IV, we analyze the effects of topography on conversion processes of atmospheric energy, and discuss interinfluence between atmospheric energy in different latitudinal zones and topographic effects on them in Section V. The mechanism of topographic effects on an increase of kinetic energy of long waves is summarized in Section VI. Summary and conclusions are given in Section VII.

## II. BRIEF DESCRIPTION OF THE MODEL AND ENERGY BUDGET EQUATIONS

The low-resolution model used for this study incorporates the spectral form of the primitive equations with a prognostic equation of moisture. The model resolution is five equally spaced sigma levels in the vertical, plus a surface level, and triangular truncation at wavenumber 10 in the horizontal. Parameterizations are included for radiation, convection, condensation, diffusion, and surface transports. Equations are solved using Galerkin procedure, and time integration is performed using a semi-implicit scheme with a time step of 90 minutes. More detailed description of the model can be found in Otto-Bliesner et al. (1982). For the model without mountains, hereafter called the NM model, the dynamical and thermodynamical equations, and physical processes are those in the model with mountains, hereafter called the M model, except for eliminating all land elevations.

The energy budget equations in one-dimensional Fourier wavenumber space (Saltzman,

1957; Perry, 1967; Baker, 1978; Otto-Bliesner, 1984) are used in this study. The variables analyzed in this paper along with symbol notations are defined in Table 1. All the computational values of the above terms are values of integration in the whole atmosphere.

Table 1. Energies and Transformations Computed in this Study

$A(n)$	available potential energy of wavenumber $n$
$A_E$	eddy available potential energy
$A_z$	zonal available potential energy
$K(n)$	kinetic energy of wavenumber $n$
$K_E$	eddy kinetic energy
$K_z$	zonal kinetic energy
$G(n)$	generation of $A(n)$
$G_E$	generation of $A_E$
$G_z$	generation of $A_z$
$D(n)$	frictional dissipation of $K(n)$
$D_E$	frictional dissipation of $K_E$
$D_z$	frictional dissipation of $K_z$
$C(n)$	conversion from $A(n)$ to $K(n)$
$C(A_E, K_E)$	conversion from $A_E$ to $K_E$
$C(A_z, K_z)$	conversion from $A_z$ to $K_z$
$M(n)$	conversion from $K(n)$ to $K_z$
$C(K_E, K_z)$	conversion from $K_E$ to $K_z$
$R(n)$	conversion from $A(n)$ to $A_z$
$C(A_E, A_z)$	conversion from $A_E$ to $A_z$
$L(n)$	rate of transfer of kinetic energy to eddies of wavenumber $n$ from eddies of all other wavenumbers
$S(n)$	rate of transfer of available potential energy eddies of wavenumber $n$ from eddies of all other wavenumbers
$BA_z$	boundary flux of $A_z$
$BA_E$	boundary flux of $A_E$
$BK_z$	boundary flux of $K_z$
$BK_E$	boundary flux of $K_E$
$BG_z$	work done by the zonal component of pressure force at the boundaries
$BG_E$	work done by the eddy component of pressure force at the boundaries

As mentioned previously, some main members, associated with the most important atmosphere phenomenon in the Northern Hemisphere during summer-planetary-scale monsoon, such as Southern Asian High, Southern Asian Low and Pacific Subtropical High, which have a significant influence on Asian climate are placed in subtropical region and the influence scope may extend to extratropical regions. Due to low resolution of the model used and the simulated Southern Asian High, Southern Asian Low and Subtropical High being to a little north of observations, the whole globe is divided into four latitudinal belts as follows:

Region 1: 81.11°S–11.53°S;

Region 2: 11.53°S–11.53°N;

Region 3: 11.53°N–46.24°N;

Region 4: 46.24°N–81.11°N.

A statistical test, i.e. the Student's test, is used to examine the climate signal in the solutions. The standard deviation of interannual variability in monthly means based on the five-year simulation of the M model is used as a measure of model variability. If the difference between monthly means in the NM model and in the M model exceeds three

standard deviations, the difference can be considered significant at the 95% confidence level or the 5% significance level (Ni et al, 1986). We use the above method to test whether the effects of topography on atmospheric energetics are statistically significant or not. Therefore, all the results and conclusions of topographic effects on atmospheric energetics in this paper are statistically significant at 5% level.

### III. THE EFFECT OF TOPOGRAPHY ON INTERACTION BETWEEN WAVES, AND BETWEEN THE ZONAL FLOW AND WAVES

Fig. 1 represents energy cycle of atmosphere in Fourier wavenumber space, where  $n$  denotes wavenumber. Fig. 2 indicates energy cycle for zonal-eddy formulation. The physical meanings of Fig. 3-Fig. 8 are the same as Fig. 1 or Fig. 2, respectively. Waves 1 through 5 are termed the long waves, and waves 6 through 10 are termed the medium waves or synoptical scale waves (Otto-Bliesner, 1984).

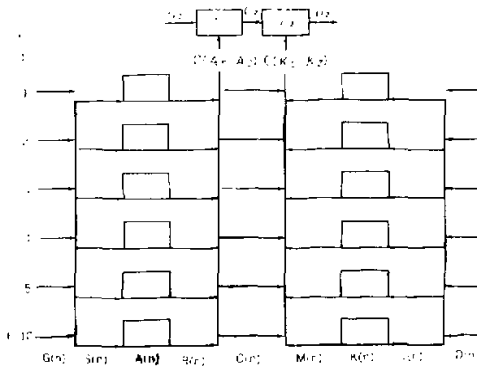


Fig. 1. Schematic box diagram of energy cycle in Fourier wavenumber space. Arrows indicate positive transformations.

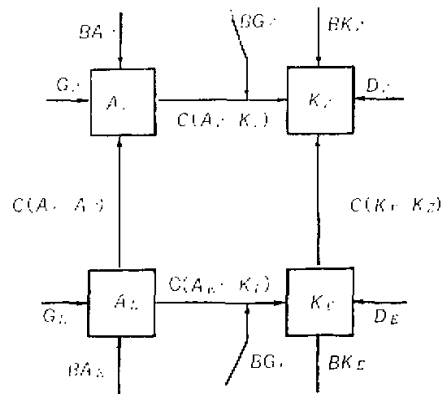


Fig. 2. Schematic box diagram of energy cycle for zonal-eddy formulation. Arrows indicate positive transformations.

Fig. 3 represents energy cycle of region 3 in the models with mountains and without mountains. Fig. 3 shows that due to non-linear interaction, long waves gain available potential energy and kinetic energy and synoptical scale waves lose them. This result differs from the conclusion (Hoskins and Pearce, 1983) which is the upscale (downscale) transfer of kinetic energy (available potential energy). But the result is in agreement with Hoskins and Pearce (1983) when the integrated area expands to  $23.31^\circ\text{N}$ - $81.11^\circ\text{N}$  (Otto-Bliesner, 1984). It suggests that transfer direction of available potential energy in region 3 is opposite to that in the latitudinal zone ( $23.21^\circ\text{N}$ - $81.11^\circ\text{N}$ ) of the Northern Hemisphere. It is because of the two main topography of the Northern Hemisphere, that is, the Tibetan Plateau and Rocky mountains lie in region 3. These two huge mountains are the important heat sources of the Northern Hemisphere during summer, especially the Tibetan Plateau. It is possible to change direction of temperature gradient in the large area (especially south side of the heat sources). Temperature advection of opposite direction generated by the local influ-

ence of topography (especially south side of the heat sources) gives rise to upscale transfer of available potential energy. Temperature advection to south of heat sources is greater than that to north of heat sources if the integrated belt is expanded toward north, downscale transfer of available potential energy is still generated. Calculation from simulation with mountains and without mountains in the 23.21°N-81.11°N latitudinal belt of the Northern Hemisphere is characterized by downscale transfer of available potential energy (see Table 2, note that the non-linear interaction term in the model without mountains is weaker than that in the model with mountains). The fact proves this point which is upscale transfer of available potential energy in region 3. It shows that influence of topography on non-linear interaction does not change direction of downscale transfer of available potential energy. The following discussed results from simulation without mountains in region 3 and in region 4 will further indicate the above point. The above results clearly show in region 3 that synoptical scale waves provide not only available potential energy to long waves, but also kinetic energy to them due to non-linear interaction between different waves. Evidently, non-linear interaction between waves is one of the energy sources maintaining long waves.

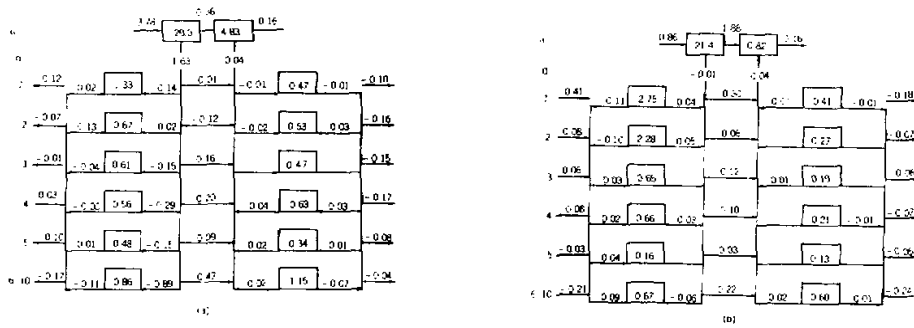


Fig. 3. Model spectral energy diagrams in July for region 3: (a) the M model; (b) the NM model. Energy in units of  $10^3 \text{ Jm}^{-2}$  and energy flux in  $\text{Wm}^{-2}$ .

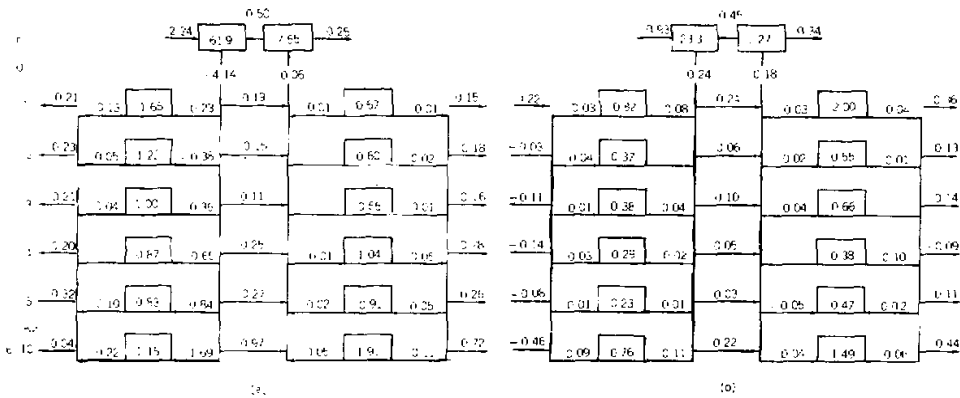


Fig. 4. As in Fig. 3 except for region 2.

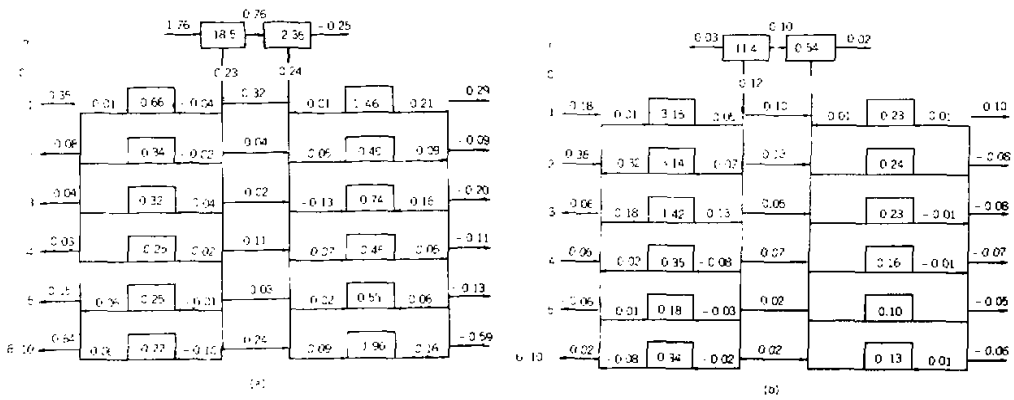


Fig. 5. As in Fig. 3 except for region 4.

It is worthy of notice that due to the interaction between all the scale waves and the zonal flow, the zonal flow transfers available potential energy to eddies and long waves of wavenumber 1 and wavenumber 2 gain kinetic energy from the zonal flow whereas eddies at wavenumber 4-10 transfer kinetic energy to the zonal flow but the latter is much greater than the former. It suggests that the zonal flow provides available potential energy of all the scale eddies but gains kinetic energy from eddies in region 3. The latter is in basic agreement with Murakami (1981). It is shown that the transfer from the zonal component of available potential energy to the eddy component is another possible energy source maintaining long

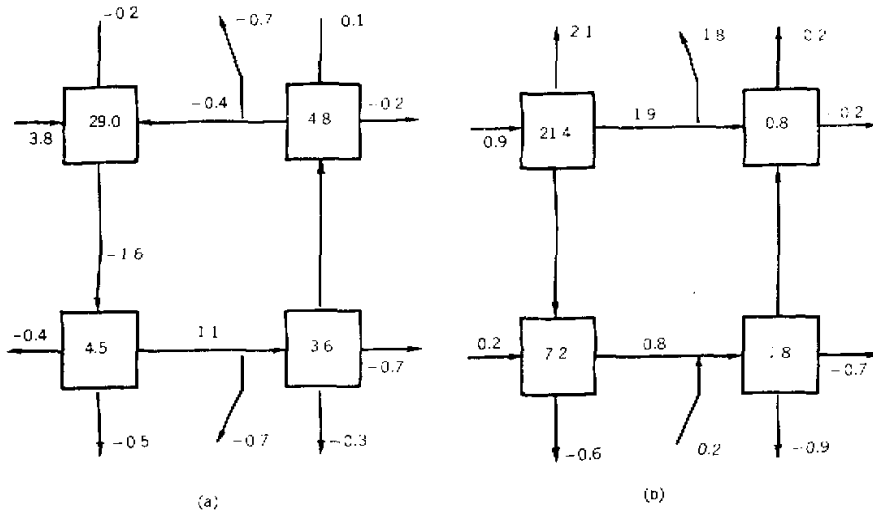


Fig. 6. Model zonal-eddy energy diagrams for region 3: (a) the M model; (b) the NM model. Energy in units of  $10^9 \text{ Jm}^{-2}$  and energy flux in  $\text{Wm}^{-2}$ .

waves in region 3. Therefore, interaction between the zonal flow and waves as a possible energy source maintaining long waves is more important than non-linear interaction between waves.

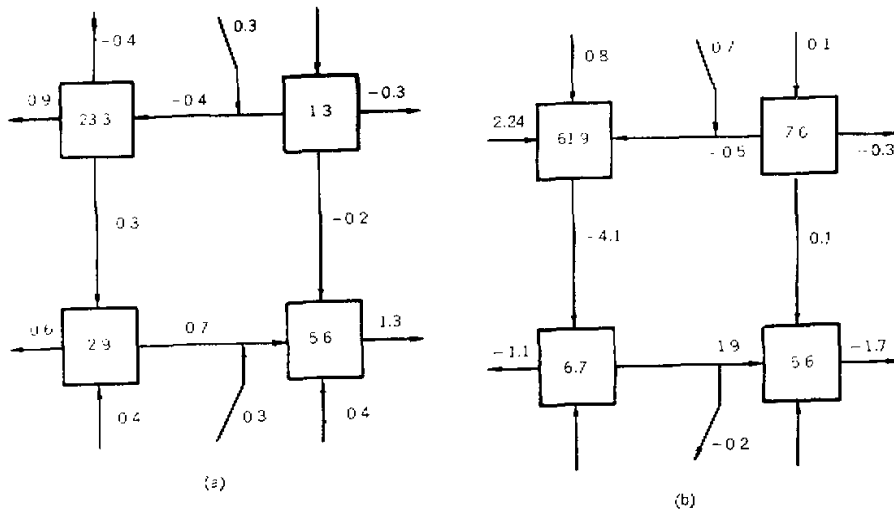


Fig. 7. As in Fig. 6 except for region 2.

The basic characteristics of energy transfer between the zonal flow and waves and between waves and waves in region 2 are similar to those in region 3 (see Fig. 4), but energy transfer between them in the equatorial region (region 2) is more evident than those in region 3. However, transfer of available potential energy from the zonal flow to eddies in the middle-high latitudes of the Northern Hemisphere (region 4) is evidently weaker than that in region 3 whereas transfer of kinetic energy between them is strengthened. It is worthy of notice that upscale transfer of kinetic energy and downscale transfer of available potential energy in region 4 comparatively agrees with Hoskins and Pearce (1983), but differs from those in region 3 and the equatorial region (region 2). The above result further shows that upscale transfer of available potential energy in region 3 results from local influence of topography.

Table 2. The Integrated Area is 23.21°N-81.11°N. Units:  $\text{Wm}^{-2}$

Wave Number	S(n)	
	with Mountains	without Mountains
1	-0.10	-0.04
2	-0.33	-0.14
3	0.02	0.07
4	0.20	0.02
5	0.01	0.03
6-10	0.13	0.01

In the NM model, transfer of available potential energy and kinetic energy caused by non-linear interaction is weak, and long waves transfer available potential energy to synoptical scale eddies. With the M model, the reverse of this happens. Interaction between the zonal flow and eddies is also weak (see Fig. 3-6).

Comparing the M model with the NM model, it may be markedly seen that interaction between waves gives rise to transferring available potential energy from synoptical scale disturbances to long waves in region 3 due to mountains; mountains also intensify interaction between the zonal flow and eddies in region 3 and increase transfer of available potential energy from the zonal flow to eddies and transfer of kinetic energy from eddies to the zonal flow.

#### IV. THE EFFECT OF TOPOGRAPHY ON CONVERSION PROCESSES OF ATMOSPHERIC ENERGY IN THE NORTHERN HEMISPHERE

It is seen that the energy conversion process  $C(A_z, K_z)$  playing an important role in maintaining mean Hadley cell mainly depends on vertical heat transport of mean meridional circulation from the energy budget equations. The barotropical conversion  $C(K_E, K_z)$  depends on north-south transport of eddy momentum and horizontal shear of the mean flow, and the baroclinic conversions  $C(A_E, K_E)$  and  $C(A_z, A_E)$  are respectively related to vertical eddy transport and north-south eddy transport of heat. Fig. 6 shows that in the M model, the baroclinic conversions from  $A_z$  to  $A_E$  and from  $A_E$  to  $K_E$  are the most important keys in the whole energy cycle. Their values are  $1.6 \text{ Wm}^{-2}$  and  $0.9 \text{ Wm}^{-2}$  respectively. It is noteworthy that the conversions from  $A_z$  to  $A_E$  and from  $A_E$  to  $K_E$  occur at all the wavenumbers. It indicates that due to the enhanced baroclinic instability, convection and eddy activities resulting in strong baroclinic conversions of energy and formation of energy conversion way, that is

$$A_z \xrightarrow{C(A_z, A_E)} A_E \xrightarrow{C(A_E, K_E)} K_E$$

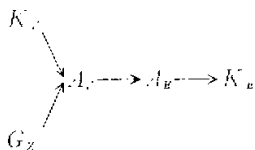
when the mountains are included. Fig. 7 and Fig. 8 also show that energy conversions in region 3 differ from those in middle-high latitudes of the Northern Hemisphere (region 4) and the equatorial region (region 2). The baroclinic conversions in region 3 are stronger than in region 4 and region 2 whereas direction of the barotropical conversion  $C(K_z, K_E)$  in region 4 and region 2 is opposite to that in region 3. Therefore, it is clear that the region where the strongest baroclinic conversions appear is region 3 in summer.

In the NM model, the conversion  $C(A_z, K_z)$  dominates with different conversion sign from the M model in region 3, that is, available potential energy of the zonal flow converts to kinetic energy of the zonal flow with decrease of baroclinic conversions, especially  $C(A_z, A_E)$ . It shows that due to the zonal symmetry of temperature gradients and decrease of north-south eddy transport of heat, the energy conversion way  $A_z \rightarrow A_E \rightarrow K_E$  is destroyed when the mountains are removed.

Comparing the M model with the NM model, it clearly suggests that topography enhances not only atmospheric instability in region 3 resulting in increasing eddy activities and cumulus convection activities, but also the zonal asymmetries of temperature gradients and diabatic heat. As a result, north-south eddy transport of heat is increased when the mountains are included. Therefore, topography enhances the baroclinic conversion  $C(A_z, A_E)$  at all the wavenumbers and  $C(A_E, K_E)$  except for wavenumber 1 in region 3 during summer. These results well agree with Ni et al. (1986). Ni et al. (1986) have



pointed out that the increase of the stationary component of  $C(A_E, K_E)$  gives rise to the increase of total baroclinic conversion  $C(A_E, K_E)$  in summer. Therefore, an important reason which the stationary component of  $K_E$  is increased is the enhancement of the stationary component of  $C(A_E, K_E)$  due to mountains. However, diabatic heating is increased and heat transport of mean meridional circulation decreased in region 3 due to the presence of topography during summer. Consequently, the generation of  $A_z$  is increased and direction of conversion  $C(A_z, K_z)$  changed, that is, conversion from  $K_z$  to  $A_z$  and the energy conversion way



is formed in region 3. All these clearly suggest that the effects of mountains on the baroclinic conversions and  $C(A_z, K_z)$  are important in region 3.

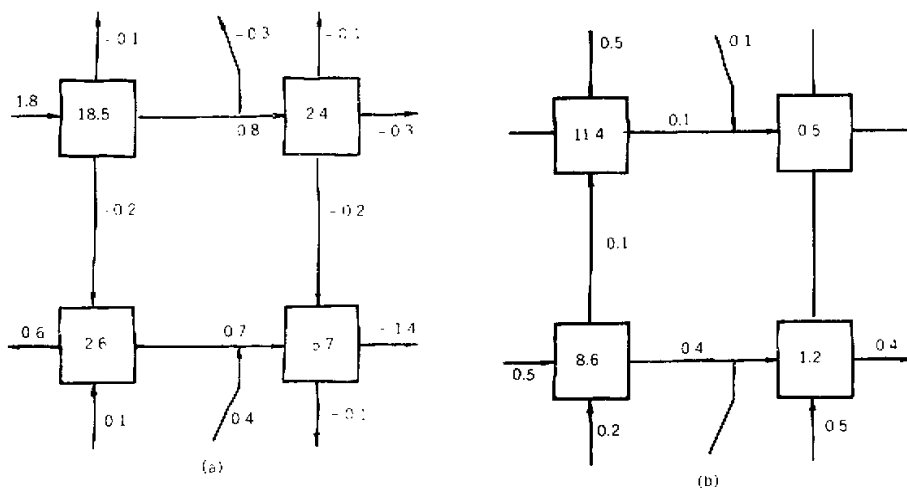


Fig. 8. As in Fig. 6 except for region 4.

V. ATMOSPHERIC ENERGY FLUXES BETWEEN LATITUDINAL ZONES

From the energy budget equations, inter-influence between latitudinal zones occurs via boundary fluxes of  $A_z$ ,  $A_E$ ,  $K_z$  and  $K_E$  and work done by boundary pressure on the inside of the region, and the increase of  $K_z$  and  $K_E$  in the region.

Fig. 9-a represents flux direction of  $A_z$ ,  $A_E$ ,  $K_z$  and  $K_E$  and sign of work done by boundary pressure. Fig. 9-a shows that  $A_z$  flux from the middle-high latitudes (region 4) to region 3 via the north boundary of region 3 exists, but  $A_z$  flux toward south at the south boundary. The former is much larger than the latter. This means that the net boundary flux of  $A_z$  toward south exists. Therefore, there is  $A_z$  flux from north to south along boundaries in July in terms of global zonal average. Flux of  $A_E$  toward north along the north boundary of region 3 and toward south at the south boundary exists. It clearly shows that region 3 is a source region in association with transport of  $A_z$  to the

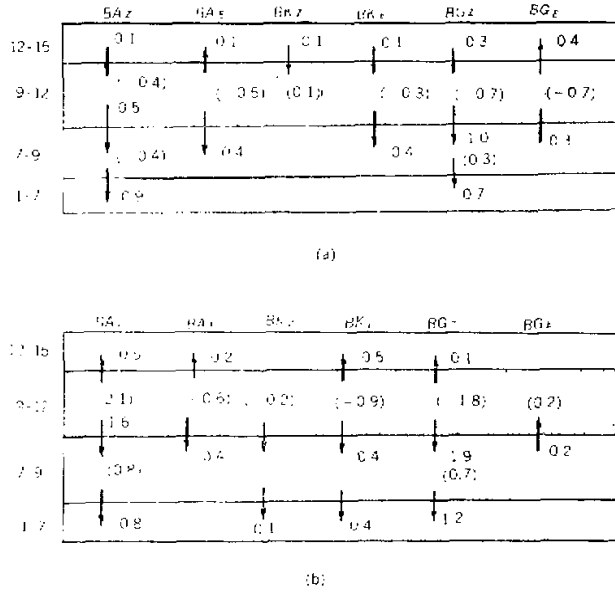


Fig. 9. Model zonal-eddy energy fluxes and work done by pressure force in four regions. 1-7 denotes region 1; 7-9 region 2; 9-12 region 3; 12-15 region 4. (a) the M model; (b) the NM model. Units:  $Wm^{-2}$ .

middle-high latitudes of the Northern Hemisphere and the equatorial region. The boundary flux of  $K_E$  differs from  $A_Z$  and  $A_E$ . There is  $K_Z$  flux from the middle-high latitudes of the Northern Hemisphere to region 3 although the amount is small.  $K_E$  is transported from the north to the south in the Northern Hemisphere, but  $K_E$  flux toward south at the south boundary is greater than that at the north boundary in region 3. Therefore, region 3 provides eddy kinetic energy to the equatorial region.  $BG_Z$  is similar to  $BA_Z$ . Region 4 provides the zonal kinetic energy to region 3 via work done by boundary pressure, but  $BA_Z$  is greater than  $BG_Z$ .  $BG_E$  is also similar to  $BA_E$ . Region 3 provides  $K_E$  to region 4 and region 2 via work done by boundary pressure. What mentioned above suggests that transport of  $K_E$  to the equatorial region (region 2) in the Northern Hemisphere and work done by boundary pressure increases  $K_E$  in region 2 resulting in gaining eddy kinetic energy and maintaining eddy activities in the equatorial region. These results are in agreement with calculation and analysis of observations by Murakami (1981). In conclusion, energy fluxes from the north to the south along boundaries dominate in July in the M model, that is, fluxes from summer hemisphere to winter hemisphere and region 3 is an energy source region. Note that region 3 provides  $A_Z$ ,  $A_E$ ,  $K_Z$  and  $K_E$  to the equatorial region (region 2).

Fig. 9-b represents flux direction of energy at boundaries and sign of work done by boundary pressure in the NM model. Fig. 9-b clearly shows fluxes of  $A_E$ ,  $A_Z$ ,  $K_Z$  and  $K_E$  from region 3 to the south and to the north via boundaries in the NM model. This means that region 3 also provides energy to the middle-high latitudes of the Northern Hemi-

sphere (region 4) and the equatorial region (region 2) in the NM model.

Comparison of the M model with the NM model indicates that energy flux direction of the north boundary is changed in region 2. Flux toward north in the NM model is changed as toward south in the M model. Obviously, the mountains prevent energy fluxes toward north and decrease them toward south. It is especially pointed out that in July, region 3 is energy source region with providing energy to the equatorial region (region 2) in either the M model or the NM model, although the middle-high latitudes of the Northern Hemisphere (region 4) also provide energy to region 3 and the former is greater than the latter. Therefore, the behavior of region 3 as an energy source region is not caused by influence of topography, but is a seasonal characteristic caused by seasonal variation of solar radiation and land-ocean contrasts.

#### VI. THE EFFECTS OF TOPOGRAPHY ON THE TRANSPORT MECHANISM OF ATMOSPHERIC ENERGY IN THE NORTHERN HEMISPHERE DURING SUMMER

According to the energy budget of region 3 in the M and the NM model, the effects of topography on energy cycle of summer atmosphere may be summarized as Fig. 10.

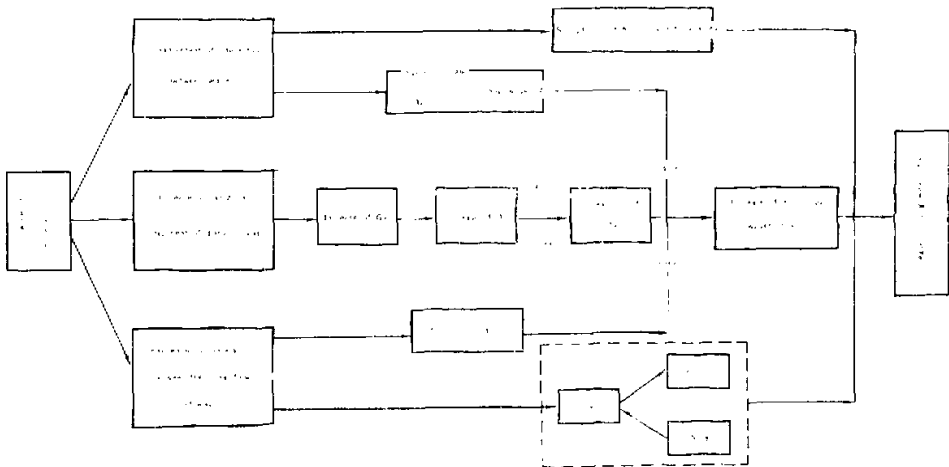


Fig. 10. Schematic diagram of the mechanism affecting kinetic energy of long waves by mountains in region 3 (41.53°N-46.24°N) during summer.

Fig. 10 shows that there are three ways to affect eddy kinetic energy at low wavenumbers (long waves) by mountains in region 3 during summer, that is: 1) interaction between waves gives rise to the transfer of  $A_E$  and  $K_E$  from synoptical scale waves to long waves resulting in increasing  $A_E$  and  $K_E$  of long waves partly in region 3 when topography is included; 2) mountains enhance interaction between the zonal flow and waves and give rise to converting  $A_Z$  to  $A_E$  and transferring kinetic energy from the zonal flow to waves at wavenumber 1 and 2; 3) mountains increase diabatic heating resulting in increasing  $A_Z$ , then finally converting to  $K_E$  via the baroclinic conversions enhanced by topography.

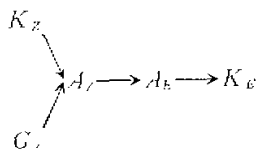
These results clearly indicate that topography markedly increases the provision of eddy kinetic energy of long waves in region 3 and further identify Ni et al. (1984)'s conclusion which Tibetan Plateau only has an influence on intensity and position of summer Asian monsoon circulation, and have shed much light upon the mechanism affecting some members of summer monsoon circulation by mountains.

## VII. CONCLUSIONS

In this paper, each term of the energy budget equations is calculated according to the simulation using the global spectral models with mountains and without mountains and their results are compared with each other. The main results of this study are:

1) Interaction between waves gives rise to transferring available potential energy and kinetic energy from synoptical scale disturbances to long waves in region 3. When topography is included, mountains increase interaction between the zonal flow and waves resulting in enhancing conversion of kinetic energy from eddies to the zonal flow.

2) Topography enhances atmospheric baroclinity and diabatic heating in region 3. Therefore, topography increases baroclinic conversions of atmospheric energy  $C(A_L, A_E)$ ,  $C(A_T, K_T)$  and generation of  $A_Z$ , and changes conversion direction of  $C(A_Z, K_Z)$  resulting in converting  $K_Z$  to  $A_Z$ , forming the conversion way of energy:



Consequently, waves at almost all wavenumbers gain kinetic energy.

3) Mountains prevent energy fluxes toward north and decrease fluxes toward south. Energy fluxes from region 3 to the equatorial region (region 2) always exist via the south boundary of region 3 in either the M model or the NM model. Therefore, behavior of region 3 as summer energy source region is seasonal characteristic caused by seasonal variation of solar radiation and land-ocean contrasts but not relative to influence of mountains.

4) Presence of mountains evidently increases the provision of eddy kinetic energy of long waves.

This research was sponsored by the Climate Dynamics Research Division, National Science Foundation through NSF Grant ATM 81-13464. Computing support by the National Center for Atmospheric Research, U.S. is gratefully acknowledged. NCAR is sponsored by the National Science Foundation, U.S.

## REFERENCES

- Baker, W.E., E.C. Kung, and R.C.J. Somerville, (1978), An energetics analysis of forecast experiments with the NCAR general circulation model, *Mon. Wea. Rev.*, **106**:311-323.
- Hoskins, B., and R. Pearce, (1983), Large-scale dynamical processes in the atmosphere, Academic Press, London.
- Kasahara, A., and W.M. Washington, (1971), General circulation experiments with a six-layer NCAR model, including orography, cloudiness and surface temperature calculation, *J. Atmos. Sci.*, **28**:657-701.
- Kasahara, A., T. Sasamori, and W.M. Washington, (1973), Simulation experiments with a 12-layer stratospheric global circulation model. I. dynamical effect of the earth's orography and thermal influence of continentality. *J. Atmos. Sci.*, **30**:1229-1251.
- Krishnamurti, T.N., (1981), Tropical Meteorology, WMO No. 364.
- Manabe, S., and T.B. Terpstra, (1974), The effects of mountains on the general circulation of the atmosphere

- identified by numerical experiments, *J. Atmos. Sci.*, **31**:3-42.
- Murakami, T., (1981), Summer mean energetics for standing and transient eddies, in the wavenumber domain, Monsoon dynamics edited by S.J. Lightill and P.R.P. Pearce, Cambridge University Press.
- Ni Yun-Qi, B.L., Otto-Bliesner and D.D. Houghton, (1984), Simulation capability and sensitivity of the regional circulation to orography in the low resolution spectral model: the summer Asian monsoon circulation.
- Ni Yun-Qi, B.L., Otto-Bliesner and D.D. Houghton, (1986), The effects of topography on the simulated atmospheric energetics in a low resolution spectral model. *J. Atmos. Sci.*, **43**:1535-1543.
- Otto-Bliesner, B.L., G.W. Branstator and D.D. Houghton, (1982), A global low-order spectral general circulation model, Part I: Formulation and seasonal climatology, *J. Atmos. Sci.*, **39**: 929-947.
- Otto-Bliesner, B.L., (1984), A global low-order spectral general circulation model, Part II: Diagnostics of the seasonal energetics, *J. Atmos. Sci.*, **41**:508-523.
- Perry, J.S., (1967), Long-wave energy processes in the 1963 sudden stratosphere warming, *J. Atmos. Sci.*, **24**:539-550.
- Saltzman, B., (1970), Large scale atmospheric energetics in the wavenumber domain, *Rev. Geophys. Space Phys.*, **8**:289-302.
- Tao Shiyun, (1983), Some Problems on East Asian Monsoon, to be published.
- Wang Jizhi, (1984), Studies and Problems of Monsoon and Cross Equatorial Flow, Advances in Synoptical Meteorology, Meteorological Press, 295-308.
- Webster, P.J., et al. (1978), Mechanisms affecting the state, evolution and transition of the planetary scale, Monsoon Dynamics, Birkhauser, 1463-1492.

